

Received 16 November 2021; revised 5 January 2022; accepted 24 January 2022. Date of publication 1 February 2022;  
date of current version 9 September 2022. The review of this article was arranged by Editor S. Shibata

Digital Object Identifier 10.1109/JEDS.2022.3148048

# Study of Dopant Activation in Silicon Employing Differential Hall Effect Metrology (DHEM)

ABHIJEET JOSHI<sup>ID</sup> AND BULENT M. BASOL<sup>ID</sup>, (Life Senior Member, IEEE)

Active Layer Parametrics, Scotts Valley, CA 95066, USA

CORRESPONDING AUTHOR: A. JOSHI (e-mail: ajoshi@alpinc.net)

**ABSTRACT** Differential Hall Effect Metrology (DHEM) technique was used to characterize highly n-type doped Si epi layers deposited on p-type Si wafers. Total dopant concentration, doping depth profile and post deposition annealing condition were changed for various sample sets and influence of such changes on the resistivity, mobility and carrier concentration depth profiles were studied. It was determined that samples annealed at 900 °C had higher activation compared to those annealed at 700 °C. Gradation in doping depth profiles did not result in similar gradation in resistivity values. Carrier concentration at the near-surface region was found to be lower in all samples. It is shown that electrical properties of films forming ultra-shallow junctions can be studied in detail and correlated with process parameters using DHEM data obtained at sub-nm depth resolution.

**INDEX TERMS** Depth profiling, DHEM, differential hall effect, dopant activation, electrical characterization, Van der Pauw.

## I. INTRODUCTION

In advanced node transistors the contact resistance dominates parasitic resistance and negatively impacts power consumption and speed of devices. Therefore, there is considerable effort directed towards reducing source/drain (S/D) contact resistivity below  $10^{-9}$  ohm-cm<sup>2</sup> level [1]. Increasing the carrier concentration in S/D requires development of doping and annealing techniques and evaluation of dopant activation, especially in the near-surface regions of the films. In this contribution, we present a study of active dopant depth profiles through n-type, highly doped Si films using Differential Hall Effect Metrology (DHEM) technique.

DHEM determines sheet resistance and sheet Hall coefficient as a function of depth through semiconductor layers [2]–[4]. It is based on the Differential Hall Effect (DHE) method [5], [6]. As applied to measurements on Si, the traditional DHE technique makes repeated Van der Pauw/Hall effect measurements after the electrically active thickness of the layer is reduced in steps, typically by surface oxidation followed by chemical etching in hydrofluoric acid (HF). Material thickness removed by the oxidation process is also measured by various means and the sheet resistance and sheet Hall coefficient data obtained as a

function of thickness removed can then be used to determine the depth profiles of carrier concentration, resistivity and mobility. DHE has not been very practical since it is a slow and manual method that needs multiple involves use of HF. DHEM, on the other hand, is a fully automated and relatively fast approach. It employs electrochemical means for semiconductor oxidation. Time consuming oxide removal by HF and the rinsing/drying steps applied after each oxidation process step in the DHE technique have been eliminated in DHEM, which carries out the Van der Pauw/Hall effect measurements under the oxide layers, without removing them. Calibration establishing a relationship between the thickness of the anodically formed oxide and the applied anodic voltage determines the depth scale, which is very dependable under fixed measurement conditions (20°C and standard pressure). At this time DHEM has the capability to controllably convert 2–5 Å of Si into oxide before each measurement step, which gives it a depth resolution of well below 1 nm.

## II. EXPERIMENTAL DETAILS

Four Si layers were epi-grown on p-type wafers and they were in-situ phosphorus (P)-doped. Thickness of the epi layers was about 45 nm. Dopant concentration was graded such

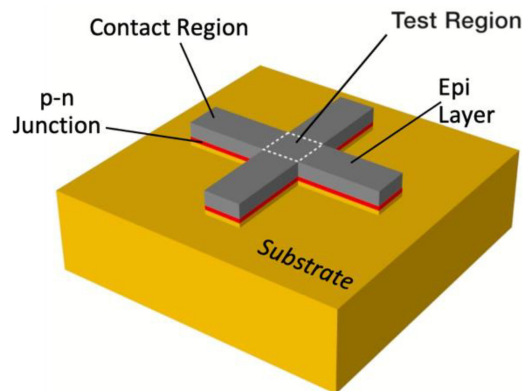


FIGURE 1. Test patterns used in DHEM measurements.

that for Samples A-700 and A-900, the doping increased from about  $2\text{E}21 \text{#/cm}^3$  at near-junction region to about  $3\text{E}21 \text{#/cm}^3$  near the surface. For Samples B-700 and B-900, the dopant profile was reversed yielding lower concentration near the surface and higher concentration in the back of the film. See the SIMS profiles for the samples in Fig. 2. After deposition, the films were annealed at  $700^\circ\text{C}$  (denoted as A-700 and B-700) and  $900^\circ\text{C}$  (denoted as A-900 and B-900) for further activation of the dopant. Cross-shaped test patterns with 1mm wide 3mm long arms were formed on the samples for DHEM measurements. A photolithography/dry etch sequence was used to form the test patterns. The dry etch process removed about 1  $\mu\text{m}$  thick material outside the cross so that the doped film within the test pattern was electrically isolated from its surroundings. The p-n junction below provided isolation from the substrate. Fig. 1 shows a drawing of the test patterns used in this work.

Before depth profiling, bulk measurements were made on the cross-shaped test patterns using Van der Pauw/Hall effect technique. Electrical contacts for these measurements were provided by four contact pins applied to the doped layer surface at the contact regions located at the ends of the cross arms. After bulk measurements, a nozzle with electrochemical process capability automatically came down and sealed against the 1mmx1mm test region (see Fig. 1) at the center of the cross, and anodic oxidation/measurement steps were initiated.

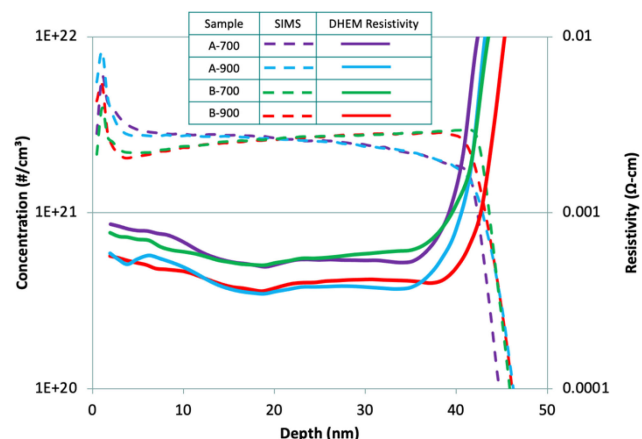
### III. RESULTS AND DISCUSSION

Results of the bulk measurements for all the samples characterized in this study are summarized in Table 1. The sheet resistance ( $R_s$ ) values, as well as the mobility ( $\mu$ ), average active dose and average active carriers are presented. A scattering factor of 1 was used for the mobility values obtained from Hall effect data.

As can be seen from Table 1, the bulk mobility and the sheet resistance values for similarly annealed samples are close. As expected, calculated active dose and average active concentration values for the  $900^\circ\text{C}$  annealed samples are higher than the  $700^\circ\text{C}$  annealed samples. Although

TABLE 1. Bulk  $R_s$ ,  $\mu$ , active dose and average carriers for sample a and sample b, annealed at different temperatures. SIMS profiles in Fig. 2.

Sample ID	A-700	A-900	B-700	B-900
Anneal	$700^\circ\text{C}$	$900^\circ\text{C}$	$700^\circ\text{C}$	$900^\circ\text{C}$
$R_s (\Omega/\square)$	148.3	100.3	142.7	98.5
$\mu (\text{cm}^2/\text{V-s})$	53.3	42.3	52.5	43.4
Dose <sub>active</sub> (#/ $\text{cm}^2$ )	$7.89\text{e}14$	$14.71\text{e}14$	$8.33\text{e}14$	$14.60\text{e}14$
Ave. <sub>active</sub> (#/ $\text{cm}^3$ )	$1.75\text{e}20$	$3.27\text{e}20$	$1.85\text{e}20$	$3.24\text{e}20$

FIGURE 2. Resistivity depth profiles of Samples A and B annealed at  $700^\circ\text{C}$  and  $900^\circ\text{C}$ , measured by DHEM. SIMS profiles show the total dopant concentrations.

the bulk data gives effective values of electrical parameters, their depth dependence can only be studied using a technique like DHEM.

Fig. 2 shows the resistivity depth profiles obtained by DHEM from all the samples. SIMS profiles of the P dopant are also given for all experimental conditions. It should be noted that unlike SIMS, DHEM data starts at the native oxide/Si interface since no real data can be collected when all or part of the applied electrochemical oxidation potential appears across the native oxide. Junction depth agrees well with the SIMS measurement suggesting that the depth calibration of DHEM for Si is good. The variation in the DHEM depth-scale (for B-900 for instance) is within the expected variation between SIMS and DHEM depth calibrations (within  $+/-10\%$ ).

As can be seen from Fig. 2, there is not much difference between the total dopant distributions for  $700^\circ\text{C}$  or  $900^\circ\text{C}$  annealing as shown by SIMS. However, resistivity clearly gets reduced for samples annealed at the higher temperature. There is also gradation in the resistivity for

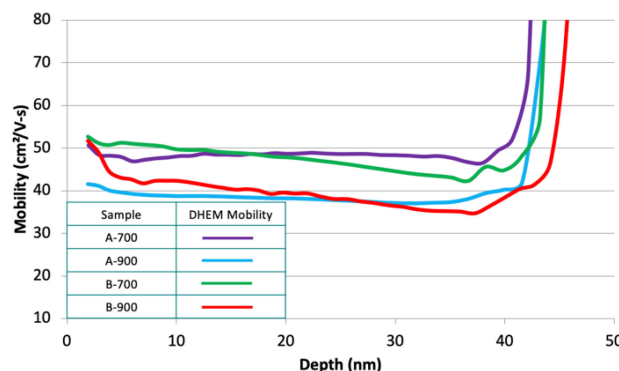


FIGURE 3. Mobility depth profiles measured by DHEM.

all samples, near surface areas showing higher resistivity values. For the 700°C annealed samples the resistivity goes from  $7.5 - 9 \times 10^{-4}$  Ω-cm near the surface to about  $5 - 6 \times 10^{-4}$  Ω-cm level deeper in the material. For the 900°C annealed samples, on the other hand, near surface resistivity is about  $6 \times 10^{-4}$  Ω-cm and it goes down to  $4 - 4.5 \times 10^{-4}$  Ω-cm level deeper in the material. Although the overall behavior of the data is similar for samples annealed similarly, there is a distinct trend in comparing the A-700 and B-700 data sets. Sample A-700 has higher resistivity compared to B-700 in the top 10nm region of the film and it has lower resistivity at the 30–35 nm deep section. It should be noted that A samples have higher dopant concentration near the surface region compared to B samples, and the reverse is true for the deeper section of the samples. Higher dopant density and higher resistivity in the surface region of the A-700 sample may suggest lower mobility due to neutral impurity scattering near the surface region. However, in general it is clear that the slight gradient in the dopant distribution as shown by the SIMS data did not greatly affect the resistivity depth profiles in these samples.

Mobility depth profiles are shown in Fig. 3. The first observation that can be made from this data is the lower mobility values observed for the samples annealed at 900°C. This is expected since the higher temperature would activate more dopants and ionized dopant scattering would also be higher. Another trend is also apparent within the same-temperature data sets. Near surface mobility is higher for B samples compared to A samples, for the same annealing temperature. As described before, B samples have lower total dopant concentration near the surface compared to A samples. This correlates well with the behavior of the mobility.

Fig. 4 shows the carrier concentration depth profiles obtained from DHEM. As expected, samples annealed at 900°C has higher activation (peak carrier concentration of  $4.7 \times 10^{21} \text{ #}/\text{cm}^3$ ) than the ones annealed at 700°C (peak carrier concentration of  $2.6 \times 10^{21} \text{ #}/\text{cm}^3$ ). Furthermore, for all samples, activation in the top 15nm region was found to be lower irrespective of the gradation in the total dopant density. Comparing the A-700 sample data with B-700, somewhat

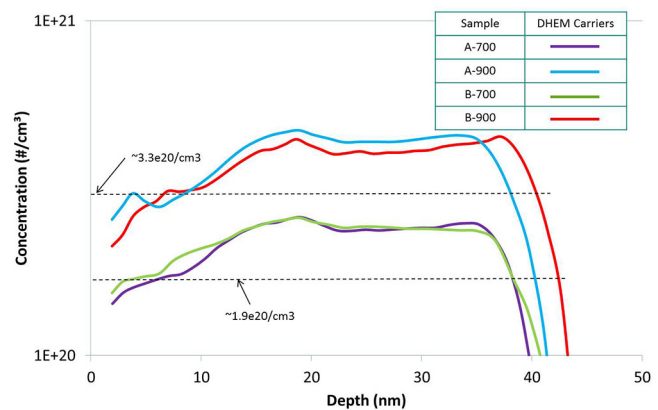


FIGURE 4. Carrier concentration depth profiles measured by DHEM.

TABLE 2. Comparison of directly measured and DHEM profile integrated values.

SAMPLE ID	$R_s (\Omega/\square)$ INTEGRATED	$\mu (\text{CM}^2/\text{V-SEC})$ INTEGRATED
A-700	151.0	48.9
A-900	105.6	38.5
B-700	149.8	47.8
B-900	102.3	39.7

higher carrier concentration values can be observed for Sample B-700 in the top 10nm region of the film. This is the region where B-700 sample has higher mobility, lower resistivity and lower total dopant concentration compared to A-700 sample. Clearly, for A-700 sample, higher total dopant concentration near the surface did not translate into lower resistivity and higher carrier concentration.

Table 2 presents the bulk values of sheet resistance and mobility which were calculated from the DHEM data. Bulk sheet resistance calculations involved integration of the resistivity profiles through the thickness of the layers. For the mobilities a similar calculation was done, however, this time taking into account the fact that in films with non-uniform mobility depth profiles, the effective mobility is given by the equation,

$$\mu_{eff} = \frac{\int n(z) \cdot \mu(z)^2 dz}{\int n(z) \cdot \mu(z) \cdot dz},$$

where  $n(z)$  and  $\mu(z)$  are the variation of carriers and mobility as a function of depth  $z$  respectively.

As can be seen from Table 2 the calculated values for sheet resistance are within  $+/-5\%$  of measured values, while mobility values are within  $+/-10\%$  that of the values given in Table 1.

#### IV. CONCLUSION

DHEM was used to generate depth profiles of resistivity, mobility and carrier concentration through highly P-doped Si epi layers. Better activation of dopants was clearly observed when the annealing temperature was raised from 700°C to 900°C. Under the experimental conditions employed, slight gradation of the total dopant concentration through the films did not directly translate into higher carrier concentration values in regions with the higher dopant content. In fact, for the 700°C annealed samples, the surface region with lower doping yielded higher mobility, lower resistivity and higher carrier concentration. Through this work it has been demonstrated that it is possible to study electrical parameters of doped films in great detail and to correlate these parameters with processing conditions, using DHEM data with sub-nm depth resolution.

#### REFERENCES

- [1] F. Khaja, "Contact resistance improvement for advanced logic by integration of EPI, implant and anneal innovations," *MRS Adv.*, vol. 4, no. 48, pp. 2559–2576, 2019.
- [2] A. Joshi and B. Basol, "ALPro system: An electrical profiling tool for ultra-thin film characterization," in *Proc. Int. Conf. Front. Characterization Metrol. Nanoelectron.*, Monterey, CA, USA, Mar. 2017, pp. 170–172.
- [3] A. Joshi, S. Novak, and B. Basol, "Differential Hall effect metrology for depth profiling of electrical properties at high resolution," in *Proc. Int. Conf. Front. Characterization Metrol. Nanoelectron.*, Monterey, CA, USA, Apr. 2019, pp. 187–189.
- [4] P. Ramesh, K. Saraswat, A. Joshi, B. Basol, L. Wand, and T. Buyuklimanli, "Differential Hall effect metrology sub-Nm profiling and its application to dopant activation in n-Type Ge," *ECS Trans.*, vol. 97, no. 3, pp. 75–80, 2020.
- [5] J. Mayer, O. Marsh, G. Shifrin, and R. Baron, "Ion implantation of silicon- II. Electrical evaluation using Hall effect measurements," *Can. J. Phys.*, vol. 45, pp. 4073–4089, Dec. 1967.
- [6] R. Galloni, G. Gavina, R. Lotti, and A. Piombini, "Automated system for the controlled stripping of thin silicon layers," *Revue de Physique Appliquée*, vol. 13, no. 2, pp. 81–84, 1978.